**Atmospheric
Chemistry
and Physics**

On the vertical distribution of boundary layer halogens over coastal Antarctica: implications for O_3, HO_x, NO_x and the Hg lifetime

A. Saiz-Lopez[1,2], **J. M. C. Plane**[1], **A. S. Mahajan**[1], **P. S. Anderson**[3], **S. J.-B. Bauguitte**[3], **A. E. Jones**[3], **H. K. Roscoe**[3], **R. A. Salmon**[3], **W. J. Bloss**[1,*], **J. D. Lee**[1,**], and **D. E. Heard**[1]

[1]School of Chemistry, University of Leeds, Leeds, UK
[2]NASA Jet Propulsion Laboratory, California Institute of Technology, Pasadena, California, USA
[3]British Antarctic Survey, National Environment Research Council, Cambridge, UK
[*]now at: School of Geography, Earth & Environmental Sciences, University of Birmingham, Edgbaston, Birmingham, UK
[**]now at: Department of Chemistry, University of York, Heslington, York, UK

Abstract. A one-dimensional chemical transport model has been developed to investigate the vertical gradients of bromine and iodine compounds in the Antarctic coastal boundary layer (BL). The model has been applied to interpret recent year-round observations of iodine and bromine monoxides (IO and BrO) at Halley Station, Antarctica. The model requires an equivalent I atom flux of $\sim 10^{10}$ molecule cm^{-2} s^{-1} from the snowpack in order to account for the measured IO levels, which are up to 20 ppt during spring. Using the current knowledge of gas-phase iodine chemistry, the model predicts significant gradients in the vertical distribution of iodine species. However, recent ground-based and satellite observations of IO imply that the radical is well-mixed in the Antarctic boundary layer, indicating a longer than expected atmospheric lifetime for the radical. This can be modelled by including photolysis of the higher iodine oxides (I_2O_2, I_2O_3, I_2O_4 and I_2O_5), and rapid recycling of HOI and INO_3 through sea-salt aerosol. The model also predicts significant concentrations (up to 25 ppt) of I_2O_5 in the lowest 10 m of the boundary layer. Heterogeneous chemistry involving sea-salt aerosol is also necessary to account for the vertical profile of BrO. Iodine chemistry causes a large increase (typically more than 3-fold) in the rate of O_3 depletion in the BL, compared with bromine chemistry alone. Rapid entrainment of O_3 from the free troposphere appears to be required to account for the observation that on occasion there is little O_3 depletion at the surface in the presence of high concentrations of IO and BrO. The halogens also cause significant changes to the vertical profiles of OH and HO_2 and the NO_2/NO ratio. The average Hg^0 lifetime against oxidation is also predicted to be about 10 h during springtime. An important result from the model is that very large fluxes of iodine precursors into the boundary layer are required to account for the observed levels of IO. The mechanisms which cause these emissions are unknown. Overall, our results show that halogens profoundly influence the oxidizing capacity of the Antarctic troposphere.

1 Introduction

Reactive halogen species (RHS=X, X_2, XY, XO, OXO, HOX, XNO_2, $XONO_2$ where X, Y is a halogen atom: Br, Cl, or I) play important roles in a number of atmospheric processes. One major impact is the depletion of ozone through catalytic cycles involving halogen radicals (e.g. Br, IO, BrO, Cl). In the 1970s, interest was focused mainly on stratospheric ozone depletion (e.g. Molina and Rowland, 1974; Stolarsky and Cicerone, 1974), whereas since the 1980s there have been reports of complete O_3 depletion events (ODEs) in the polar tropospheric boundary layer (BL) of both the Arctic and Antarctic (e.g., Bottenheim et al., 1986; Oltmans and Komhyr, 1986; Murayama et al., 1992; Kreher et al., 1997; Tuckermann et al., 1997; Wessel et al., 1998; Spicer et al., 2002; Brooks et al., 2006; Jones et al., 2006). These events occurred at polar sunrise in the spring and were explained by the influence of bromine-catalyzed chemical cycles (e.g. Barrie et al., 1988; McConnell et al., 1992; Tuckermann et al., 1997; Kreher et al., 1997; Frieß et al., 2004; Kaleschke et al., 2004). Bromine chemistry also plays a central role in the oxidation of atomic mercury (Hg^0) in the polar atmosphere (Schroeder et al., 1998; Brooks et al., 2006), which seems to provide an important pathway for this element to enter

Correspondence to: J. M. C. Plane
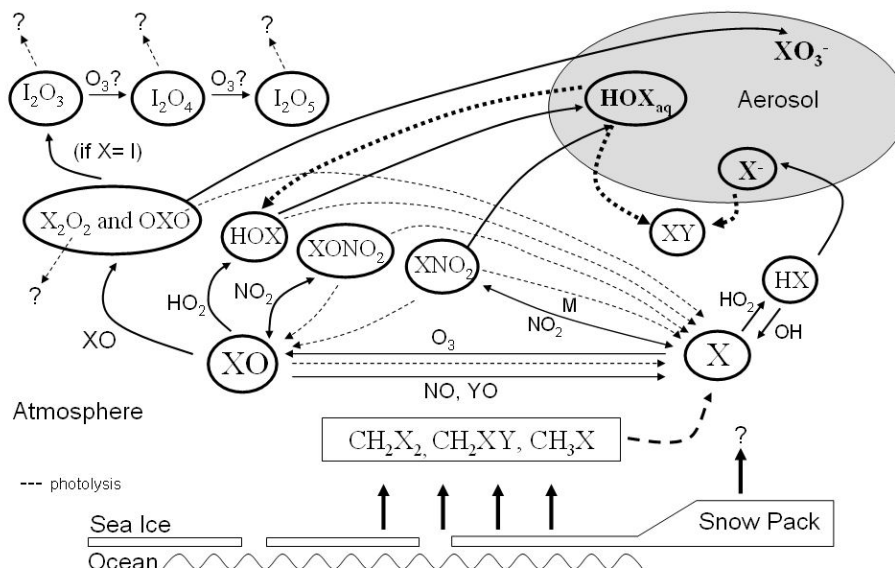(j.m.c.plane@leeds.ac.uk)

Fig. 1. Simplified scheme of bromine and iodine chemistry in the Antarctic boundary layer.

the Arctic food chain (Scott, 2001). It has been suggested that the presence of iodine can trigger this bromine chemistry and enhance the removal of ozone and mercury (Sander et al., 1997; Calvert and Lindberg, 2004a, b; O'Driscoll et al., 2006).

Major components of the atmospheric chemistry of bromine and iodine in the polar BL are illustrated in Fig. 1. The release of bromine-containing compounds proceeds through the so-called "bromine explosion", which involves bromide ions in brine-coated sea ice or snow being converted to gas-phase inorganic bromine (Br, BrO, HOBr etc.) in the BL (Hönninger and Platt, 2002). The presence of BrO has been reported by several groups such as Tuckermann et al. (1997) at Ny Ålesund, Hönninger et al. (2004a) at Hudson Bay, Canada and Brooks et al. (2006) at Barrow, Alaska. Ground-based measurements of BrO have also been made in coastal Antarctica using a passive differential optical absorption spectrometer (DOAS) during the spring of 1999 and 2000 (e.g. Frieß et al., 2004). Satellite observations have shown the presence of BrO in both the northern and southern polar regions (Richter et al., 1998; Wagner and Platt, 1998; Wagner et al., 2001; Richter et al., 2002; Hollwedel et al., 2004).

The vertical extent of bromine chemistry has been studied using a combination of the long path DOAS and multi-axis DOAS measurement techniques (Tuckermann et al., 1997; Martinez et al., 1999; Hönninger et al., 2004b). These studies showed that the enhanced BrO during ODEs was confined to the BL. It was also concluded that there was a very small vertical gradient of BrO within the BL (Hönninger and Platt, 2002; Hönninger et al., 2004b). These observations of BrO being well-mixed within the BL are consistent with a

one-dimensional model study by Lehrer et al. (2004), which concluded that ODEs in the Arctic are caused by halogen chemistry confined to the BL by an inversion layer. This study also showed that emission from brine-covered sea ice was not sufficient to explain the observed ODEs, and suggested that recycling of halogen radicals through heterogeneous chemistry on aerosols was also required. A multiphase model study of bromine chemistry at polar sunrise concluded that O_3 depletion cannot be simulated without the presence of heterogeneous halogen chemistry involving the snowpack (Michalowski et al., 2000).

Besides removing O_3, RHS can also affect the oxidizing capacity of the troposphere in other ways. X and XO radicals reach a photochemical steady state during the day, essentially governed by reaction with O_3 and photolysis (Fig. 1). The X atoms can react with non-methane hydrocarbons (NMHC), leading to hydrogen atom abstraction (analogous to OH). In fact, indirect measurements of the vertical extent of RHS have been carried out by measuring hydrocarbon destruction patterns (Solberg et al., 1996; Ramacher et al., 1999). Br atoms also recombine with Hg^0 to produce HgBr, which is relatively stable at the low temperatures of the polar spring BL; HgBr can then add a further radical (Br, I etc.) to yield mercury in its stable +2 oxidation state (Goodsite et al., 2004). Halogen oxides such as BrO and IO can also act directly as oxidizing radicals. For example, the rate of oxidation of dimethyl sulphide (DMS) by BrO can be up to an order of magnitude higher than the oxidation by OH (Saiz-Lopez et al., 2004; von Glasow et al., 2004).

RHS also affect the HO_x (i.e., $[HO_2]/[OH]$) and NO_x ratios (i.e., $[NO_2]/[NO]$) (e.g. von Glasow and Crutzen, 2003; Saiz-Lopez and Plane, 2004a; Bloss et al., 2005). XO

radicals oxidize NO to NO_2, thus increasing the NO_x ratio. In contrast, they react with HO_2 to yield HOX, which then photolyses efficiently to OH (particularly in the case of HOI), thus decreasing the HO_x ratio (Bloss et al., 2005). A detailed study of BrO_x-ClO_x-HO_x-NO_x chemistry during bromine-catalysed ozone depletion events in the Arctic boundary layer has been performed by Evans et al. (2003).

Lastly, the role of iodine oxides in forming ultra-fine aerosol has been investigated by laboratory, field and modeling experiments (e.g. O'Dowd et al., 1998; Hoffmann et al., 2001; O'Dowd et al., 2002; Jimenez et al., 2003; Saiz-Lopez and Plane, 2004b; McFiggans et al., 2004; Burkholder et al., 2004; Sellegri et al., 2005; Saunders and Plane, 2005, 2006; Saiz-Lopez et al., 2006). The process of iodine oxide particle (IOP) production is thought to involve the recombination reactions IO+IO, IO+OIO, and OIO+OIO to yield I_2O_y, where y=2, 3 or 4, respectively. Further oxidation with O_3 may then produce the most stable higher oxide, I_2O_5, which can then polymerize to form solid particles of I_2O_5 (Saunders and Plane, 2005, 2006). Thus the presence of IO in the atmosphere points to the possibility of IOP formation; these particles could then provide condensation nuclei for other condensable vapours and grow to the point of becoming cloud condensation nuclei.

In Antarctica, the vertical column of IO was measured over a year using a ground-based differential optical absorption spectrometer (DOAS) (Frieß et al., 2001), and very recently from the SCIAMACHY instrument on the ENVISAT satellite (Saiz-Lopez et al., 2007b; Schönenhardt et al., 2007). However, the most comprehensive dataset of direct measurements of Antarctic IO (and BrO) in the BL was obtained during the Chemistry of the Antarctic Boundary Layer and Interface with Snow (CHABLIS) field measurement campaign at Halley Station, shown on the map in Fig. 2 (Saiz-Lopez et al., 2007a). In the present paper we investigate, using a 1-D model, the source strengths and likely vertical distributions of halogens within the Antarctic BL. The effects of the combined iodine and bromine chemistry on O_3 depletion, the HO_x and NO_x ratios and the lifetime of Hg within the BL are then explored.

2 Model description

The Tropospheric Halogen Chemistry model (THAMO) is a one-dimensional chemical and transport model that uses time-implicit integration (Shimazaki, 1985). It has three main components: i), a chemistry module that includes photochemical, gas-phase and heterogeneous reactions; ii), a transport module that includes vertical eddy diffusion; and iii), a radiation scheme which calculates the solar irradiance as a function of altitude, wavelength and solar zenith angle. The continuity equations to account for the change in con-
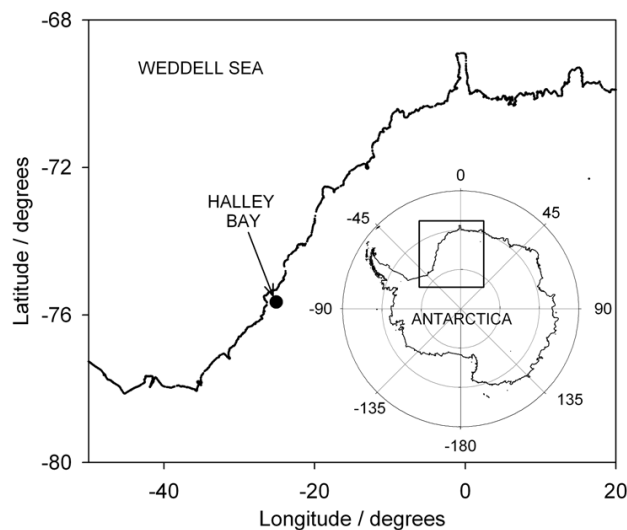

Fig. 2. Map showing the location of Halley Station on the Brunt Ice Shelf in Antarctica during 2005. Antarctic coastline generated using the Coastline Extractor page hosted by the National Oceanic & Atmospheric Administration (NOAA)/National Geophysical Data Center, Marine Geology and Geophysics Division.

centration n_i of a species i at an altitude z and a time t are given by:

$$\frac{\partial n_i}{\partial t} = P_i - L_i n_i - \frac{\partial \phi_i}{\partial z} \qquad (1)$$

where P_i and L_i are the production and loss rates of species i, respectively. ϕ_i is the vertical flux due to eddy diffusion:

$$\phi_i = K_z \left[\frac{\partial n_i}{\partial z} + \left(\frac{1}{T} \frac{\partial T}{\partial z} + \frac{1}{\overline{H}} \right) n_i \right] \qquad (2)$$

where $\overline{H}$ is the scale height of the atmosphere and K_z is the eddy diffusion coefficient (the second and third terms in Eq. (2) cast the flux in terms of the vertical gradient in mixing ratio, rather than just concentration (Shimazaki, 1985)). These equations are solved in the model with an integration time step of 2 min, which was chosen as a compromise between computational efficiency and compliance with the Courant-Levy criterion (Courant et al., 1928): reducing the time step to 15 s changed the calculated IO and BrO after 48 h by less than 1%. In this study, the model extends from the ground up to the upper boundary at 200 m with a spatial resolution of 1 m. To account for the entrainment of free tropospheric O_3, a flux into the top-most level of the model at the upper boundary can be turned on (or set to zero for the case of a stable BL). The lower boundary is the snowpack surface, where deposition from the gas phase and an upward trace gas flux from the snowpack can occur.

2.1 Vertical transport parameterization

This is described by the turbulent diffusion coefficient $K_z(z, t)$, which will usually be a function of time t and height z. Near the surface, the layer where there is minimal change in momentum flux, turbulence is generated predominantly by wind shear. This "surface layer" is well described by Monin-Obhukov similarity theory, from which a function for the diffusion coefficient can be derived (Stull, 1988):

$$K_z(z, t) = \kappa.z.u*(t) \tag{3}$$

where κ is the von Kármán constant=0.4, z is the height above the surface and $u*(t)$ is the surface friction velocity. In the stable BL, where buoyancy can be neglected, $u*$ can be derived to a good approximation from:

$$\frac{\kappa U}{u*} = \ln\left(\frac{z}{z_0}\right) \tag{4}$$

where U is wind speed, z is the measurement height of the wind, and z_o is the surface roughness length. For Halley, long-term measurements indicate that $z_o \sim 5 \times 10^{-5}$ m (King and Anderson, 1994). Note that this form of $K_z(z, t)$ is relevant to the surface layer, where $u*(t)$ is virtually constant. Equation (4) implies that $K_z(z, t)$ is linearly dependent on z, and tends to zero at the surface. This in turn would imply that a trace gas released at the surface, $z=0$, would never diffuse upwards, a situation which is clearly unrealistic. Hence, a surface condition is used which assumes that this form of $K_z(z, t)$ is only valid for $z \geq z_o$ (Stull, 1988). The model was run for two scenarios: stable neutral conditions, where K_z decreased from 4.7×10^3 cm^2 s^{-1} at 1 m to 2.0 cm^2 s^{-1} at the top of the BL (200 m); and convective conditions, where K_z varied from 700 cm^2 s^{-1} at 1 m to 1×10^4 cm^2 s^{-1} above 30 m.

2.2 Chemical scheme

The major objective of this modelling study is to simulate the IO observations, and thus explore the impact of iodine chemistry in the polar BL. The THAMO *standard model* contains the gas-phase iodine chemistry scheme we have used in previous modelling studies (McFiggans et al., 2000; Saiz-Lopez et al., 2006). The sources of the high concentrations of halogens at Halley are an open question. In fact, an explicit investigation of the microphysical processes that occur at the ice-atmosphere interface and lead to halogen release from ice surfaces is beyond the scope of this paper. The DOAS observations of IO and BrO indicate that oceanic air from the sea ice zone provides the primary halogen source (Saiz-Lopez et al., 2007a), although there is evidence that efficient snowpack recycling provides a secondary source. The rationale for this is that during CHABLIS significant concentrations of both IO and BrO were observed in air masses that had been in the continental boundary layer for several days (Saiz-Lopez et al., 2007a). This indicates (though does not prove)

an efficient recycling of halogens following deposition onto the snowpack of either gas-phase species or wind-blown sea salt/frost flowers (since Halley is a coastal station – Fig. 2).

However, our knowledge about the details of these halogen sources is poor. Since horizontal transport is also not considered in this 1-D vertical model, we use the model to estimate the source strengths required to account for the observed IO and BrO concentrations (the model uses state-of-the-art halogen gas-phase chemistry). In order to simulate the largest concentrations of IO and BrO observed (during spring), the emission fluxes of I_2 and Br_2 from the snowpack were required to be 1×10^{10} molecule cm^{-2} s^{-1} and 1×10^9 molecule cm^{-2} s^{-1} at midday, respectively. The recycling in the snowpack is also assumed to be photochemical (for reducing iodine from the +3, +4 or +5 oxidation states). These fluxes are therefore assumed to depend on actinic flux, and hence their diurnal variation is described by a Gaussian profile peaking at midday.

Heterogeneous chemistry is treated in the following way. The uptake and subsequent hydrolysis of $IONO_2$, HOI and INO_2 on aerosols produces HOI, which equilibrates between gas and aqueous phase according to its Henry's law solubility. The processing of aqueous HOI to IBr, ICl and I_2, via reaction with Br$^-$, Cl$^-$ and I$^-$, respectively, takes only between 10 and 15 min in fresh sea-salt aerosol (McFiggans et al., 2000). The di-halogen molecules are insoluble and so are released rapidly to the gas phase. Hence, uptake of the inorganic iodine species onto aerosols is the rate-limiting step of the process (McFiggans et al., 2000). Note, however, that aged sea-salt aerosols become depleted in Br$^-$ and Cl$^-$, which will slow down the aerosol processing time. Aged aerosols also become progressively acidified by uptake of HNO_3, H_2SO_4 and SO_2 (e.g. Fickert et al., 1999; von Glasow et al., 2002) which increases the rate of processing. However, for this study we do not explicitly treat the aqueous phase chemistry in the bulk of the aerosol. Instead, we assume that the limiting step for halogen heterogeneous recycling on aerosols is the first-order rate of uptake which we compute, using the free-regime approximation, for a number of gas phase species (Table 1 of the Supplementary Material: http://www.atmos-chem-phys.net/8/887/2008/acp-8-887-2008-supplement.pdf).

The gas-phase chemistry of IO in very clean air (NO$_x$<30 ppt) is dominated by the reactions of IO with itself to form I_2O_2 and OIO+I (Sander et al., 2006), IO+OIO to form I_2O_3 (Gomez Martin et al., 2007), and OIO+OIO to form I_2O_4 (Gomez Martin et al., 2007). These reactions proceed rapidly in the gas phase with rate coefficients of $\sim 1 \times 10^{-10}$, 5×10^{-11} and 1×10^{-10} cm^3 molecule^{-1} s^{-1}, respectively. The model also includes the formation of gas-phase I_2O_5 through a series of oxidation reactions of I_2O_2, I_2O_3 and I_2O_4 by O_3 up to the +5 oxidation state; we adopt a possible lower limit to the rate coefficients of these reactions of 6×10^{-13} cm^3 molecule^{-1} s^{-1} (Saunders and Plane, 2005). We also assume in the standard model that I_2O_2,

I_2O_3, I_2O_4 and I_2O_5 do not undergo photolysis or other reactions which would reduce them to IO or OIO, and that these molecules are lost by dry deposition to the snowpack and uptake onto pre-existing aerosol surfaces. Hence, any newly formed IO and OIO will be rapidly converted into higher-order iodine oxides, effectively limiting the atmospheric lifetime of both radicals. This means that when air masses arrived at Halley directly from the sea ice – when the measured IO and BrO concentrations were significantly higher (Saiz-Lopez et al., 2007a) – any IO produced from emissions over the sea ice would not have remained in the gas phase while being transported (transit time typically 2 h). However, using the revised model chemistry where photolysis of I_xO_y is included (see below), IO could have been recycled in the gas phase during transit.

In addition to halogen chemistry, the THAMO model contains a set of odd-hydrogen, odd-nitrogen and methane chemical reactions, and a limited treatment of non-methane hydrocarbon (NMHC) chemistry. It also includes a detailed chemical scheme of reduced sulphur oxidation. Specific details of the iodine and bromine chemistry schemes are given in Sects. 4.1 and 4.2, respectively. A simplification of the chemistry described in the model is illustrated in Fig. 1, whereas the full reaction scheme is listed in Table 1 of the Supplementary Material (http://www.atmos-chem-phys.net/8/887/2008/acp-8-887-2008-supplement.pdf). The model is constrained with typical measured values of other chemical species via a time-step method. This requires that the field data were first averaged or interpolated to the two-minute frequency. Then, the concentrations of the constrained species were read in at the appropriate integration time step. Hence, these species were not assigned continuity equations and integrated, and their fluctuations do not determinate the size of the integration time-step. The species used to constrain the model were measured during the CHABLIS campaign, and had the following peak mixing ratios: [CO]=35 ppb; [DMS]=80 ppt; [SO_2]=15 ppt; [CH_4]=1750 ppb; [CH_3CHO]=150 ppt; [HCHO]=150 ppt; [isoprene]=60 ppt; [propane]=25 ppt; [propene]=15 ppt (Jones et al., 2007a; Read et al., 2007). The model is also updated at every simulation time-step with measurements of temperature and relative humidity made during CHABLIS.

2.3 Photochemistry

The rate of photolysis of species is calculated on-line using an explicit two-stream radiation scheme from Thompson (1984). The irradiance reaching the surface is computed after photon attenuation through 50 1-km layers in the atmosphere as a function of solar zenith angle (SZA), location and time-of-year. The absorption cross-section and quantum yield data used in this model are summarized in Table 1 (Supplementary Material – http://www.atmos-chem-phys.net/8/887/2008/acp-8-887-2008-supplement.pdf). The rate of photolysis of species is computed by including snowpack albedo measurements (typical measured albedo=0.85) made with an actinic flux spectrometer during the CHABLIS campaign (Jones et al., 2007a).

2.4 Sea ice/snowpack surface and aerosol uptake

Dry deposition to the surface occurs from the lowermost level of the model. Deposition was included for the following species: HOBr, HOI, HBr, HI, $IONO_2$, $BrONO_2$, OH, HO_2, NO_3, N_2O_5, CH_3O_2, HNO_3 and H_2SO_4. The deposition flux of each gaseous species i was calculated as $V_d C_i$, where V_d is the deposition velocity and C_i is the concentration of i. Deposition velocities were set to $0.5\,cm\,s^{-1}$. Here we assume that the ground is a flat surface. Similarly, the uptake of these species onto sea-salt aerosol surfaces was included in the model. The uptake of a gas species onto an aerosol surface was computed using the volumetric aerosol surface area (ASA) and the free molecular transfer approximation (Fuchs, 1964). The ASA used in this work is $10^{-7}\,cm^2\,cm^{-3}$ (von Glasow et al., 2002), chosen to be typical of remote oceanic conditions, and is assumed constant in each vertical level of the model (i.e. the aerosol is well-mixed in the BL). Note that Halley is a remote coastal station and in the absence of aerosol measurements during CHABLIS we consider this ASA is the best estimate available. The uptake coefficients (see Table 1 of the Supplementary Material – http://www.atmos-chem-phys.net/8/887/2008/acp-8-887-2008-supplement.pdf) are taken from the recommendations of Sander et al. (2006) and Atkinson et al. (2000), unless otherwise stated.

3 DOAS observations at Halley Station

BL observations of IO and BrO were carried out from January 2004 to February 2005 using the technique of long-path DOAS (Platt, 1994; Plane and Saiz-Lopez, 2006). The measurements were performed during the CHABLIS campaign at Halley Station (75°35′ S, 26°30′ W) situated on the Brunt Ice Shelf, about 35 m above sea level (Fig. 2). The ice edge is some 12 km north, 30 km west and 20 km south-west of the station. A detailed description of the CHABLIS campaign can be found elsewhere in this issue (Jones et al., 2007a).

The instrument was located in the Clean Air Sector Laboratory (CASLAB). An effective light path of 8 km at a height of 4 to 5 m above the snowpack (varying through the year as a result of snow accumulation) was set up between the CASLAB and a retro-reflector array positioned 4 km to the east. Further information on the instrumental design and spectral de-convolution procedures can be found in Plane and Saiz-Lopez (2006).

The measurements provide comprehensive observations of the diurnal and seasonal trends of both radicals at the base of the coastal Antarctic BL (Saiz-Lopez et al., 2007a). The IO and BrO concentrations exhibit a diurnal cycle with a clear
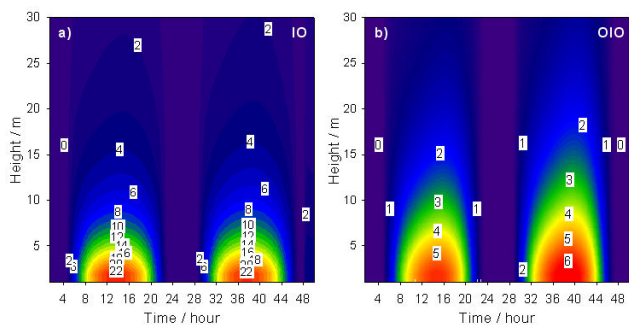
Fig. 3. Modelled diurnal variations of a), the IO mixing ratio profile, and b), the OIO mixing ratio profile during austral spring at Halley, using the standard model (see text for details). The mixing ratios at a height of 5 m agree well with the measurements made during the CHABLIS campaign using a DOAS with a beam ~5 m above the snowpack (Saiz-Lopez, 2007a).

dependence on solar irradiance. Higher concentrations were also measured in air that had passed over sea ice within the previous 24 hours. However, even in continental air that had spent at least four days over the interior of Antarctica, both radicals were still measured at mixing ratios up to ~6 ppt during sunlit periods, significantly above the detection limit of the instrument (1–2 ppt).

The seasonal trends of both radicals are remarkably similar, both in timing and absolute concentration. The radicals first appeared above the DOAS detection limit during twilight (August), and were then present throughout the sunlit part of the year. The peak mixing ratios of IO and BrO (20 ppt) were measured in springtime (October), followed by a possible smaller peak in autumn (March–April). Regarding the DOAS detection of OIO, the molecule was not conclusively measured above its DOAS detection limit (6–7 ppt) during 21 days of observations between January 2004 and February 2005. For more details about the DOAS measurements and correlation with meteorology during CHABLIS, see Saiz-Lopez et al. (2007a).

4 Results and discussion

4.1 Iodine chemistry

Here we use the model to investigate two important questions. First, what is the iodine source strength required to simulate the IO mixing ratios observed at the height of the DOAS measurements (i.e., 4–5 m above the snowpack)? Second, what is the vertical extent of the iodine chemistry in this environment: is its impact limited to the near surface or throughout the entire BL? During the CHABLIS campaign, the highest mixing ratios of IO, up to 20 ppt, were observed in springtime, following halogen activation mechanisms that, for the case of iodine, are not yet well understood.

Figure 3 shows the modelled mixing ratios of IO and OIO in spring using the standard model of iodine chemistry, with an I atom flux out of the snowpack of 1×10^{10} molecule $cm^{-2}\,s^{-1}$. The calculated IO mixing ratio maximum of 16–18 ppt is in good accord with the DOAS observations. Sunrise is at 04:30 and sunset at 23:30 GMT. The days which match these conditions during CHABLIS are 20 and 21 October 2004, which are presented in Saiz-Lopez et al. (2007a). For OIO the mixing ratios are below 6 ppt, which was the instrumental detection limit during the CHABLIS campaign. The diurnally-averaged lifetime for I_xO_y is ~2 h. The modelled summer IO mixing ratio at midday peaking at 6 ppt, in accord with the DOAS observations, requires an I atom flux out of the snowpack of 1×10^9 molecule $cm^{-2}\,s^1$.

Figure 3a and b show that both IO and OIO exhibit a strong vertical gradient in the BL: the concentration of IO at a height of 30 m is only 10% of that at 5 m. In the standard model, the transport of reactive iodine to the top of the BL occurs only via iodine recycling through sea-salt aerosol. However, the result of such a steep IO gradient is that the column abundance of the radical is predicted to be only 7×10^{11} molecule cm^{-2} for the springtime simulation in Fig. 3. This is very much smaller than satellite observations of IO by SCIAMACHY in October 2005, where vertical columns $>3 \times 10^{13}$ molecule cm^{-2} were observed over Antarctic sea ice (Saiz-Lopez et al., 2007b; Schönhardt et al., 2008), or zenith-pointing DOAS measurements of the IO slant columns up to 1×10^{14} molecule cm^{-2} made at the coastal Antarctic station of Neumayer (Frieß et al., 2001). Hence, vertical column measurements strongly suggest that IO does *not* have a steep gradient within the BL. The most likely explanation is that the standard model is missing a recycling mechanism from the higher iodine oxides to IO, which would increase the IO lifetime and allow it to be well-mixed in the BL.

The most likely recycling mechanism is photodissociation of I_xO_y. This would have two effects: i) increase the lifetime of IO_x and therefore impact on the vertical distribution of inorganic iodine, ii) reduce the required atomic I flux from the snowpack into the gas phase to sustain the observed levels of IO. The model was therefore run with the photolysis of I_2O_2, I_2O_3, I_2O_4 and I_2O_5, set to a frequency at noon of $1 \times 10^{-2}\,s^{-1}$. This photodissociation frequency is 2–3 times faster than $J(IONO_2)$ at this location in spring, calculated using a new measurement of the $IONO_2$ photolysis cross section (Joseph et al., 2007). Preliminary measurements of the absorption cross sections of these higher iodine oxides (Gomez Martin et al., 2005) indicate that their magnitudes and long wavelength thresholds are similar to those of $IONO_2$. Nevertheless, further laboratory work on the photochemistry of I_xO_y species is urgently needed to advance our understanding of this aspect of atmospheric iodine chemistry.

The inclusion of I_xO_y photolysis is now referred to as the *revised model*. Figure 4a shows the computed IO mixing ratio for the springtime scenario using the revised model
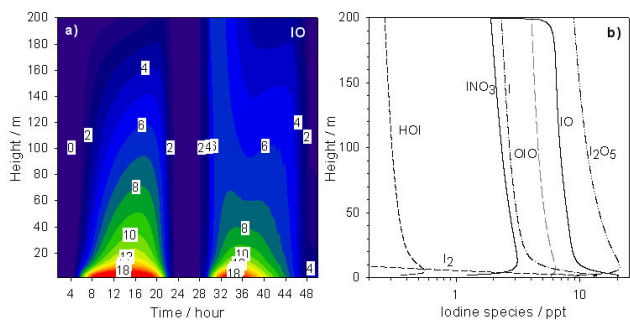
Fig. 4. (a) Modelled diurnal IO mixing ratio profile during austral spring at Halley, and **(b)** vertical profiles at noon of the main gas-phase iodine species, using the revised model (photolysis of I_xO_y). The mixing ratios at a height of 5 m agree well with the measurements made during the CHABLIS campaign using a DOAS with a beam ~5 m above the snowpack (Saiz-Lopez, 2007a).

(note the different height scale with respect to Fig. 3). The calculated IO at the top of the BL (200 m) is now 20% of that close to the surface, and the vertical column of 5×10^{12} molecule cm^{-2} is now approaching reasonable accord with the satellite column measurement. Thus, $J(I_xO_y){=}1 \times 10^{-2}$ s^{-1} is the lower limit required to sustain high IO levels throughout the boundary layer. Figure 4b shows vertical profiles of the major gas-phase iodine species throughout the BL. Note that the main reservoir of iodine is I_2O_5 with mixing ratios ranging from 25 ppt to 8 ppt from the surface to the top of the BL, respectively. Figure 5a illustrates a comparison between the measurements of IO and the model. The lack of agreement in the decrease of IO after midday may indicate that the chemistry in the model requires further development, or simply that this is a 1-D model applied to a spatially heterogeneous environment.

Figure 6 shows the modelled diurnal variation of the I_2O_5 mixing ratio. Since the formation rate of IOPs is highly non-linear in I_xO_y mixing ratio (Saunders and Plane, 2005), most ultra-fine particles are predicted to form in the first 10 m above the snowpack, in the early afternoon (12:00–16:00 LT). This may be the source of ultra-fine particles that have been measured over sea-ice around Antarctica (Davison et al., 1996). Once IOPs form, there will be a competition between uptake onto pre-existing aerosol and further growth by the uptake of condensable vapours and coagulation.

The precise mechanism by which IO and OIO form IOPs is a subject of ongoing research, and IOP formation cannot be modelled with a great degree of confidence. There are two problems. The first is that the solid particles produced in laboratory studies have the stoichiometry of I_2O_5, but it is not clear whether this is produced in the gas phase by O_3 oxidising I_2O_y (y<5), or by the polymerization of these lower oxides into particles which then rearrange and eject I_2 (Saunders and Plane, 2005). The second is that although IOP production in the laboratory is a rapid process (Burkholder et
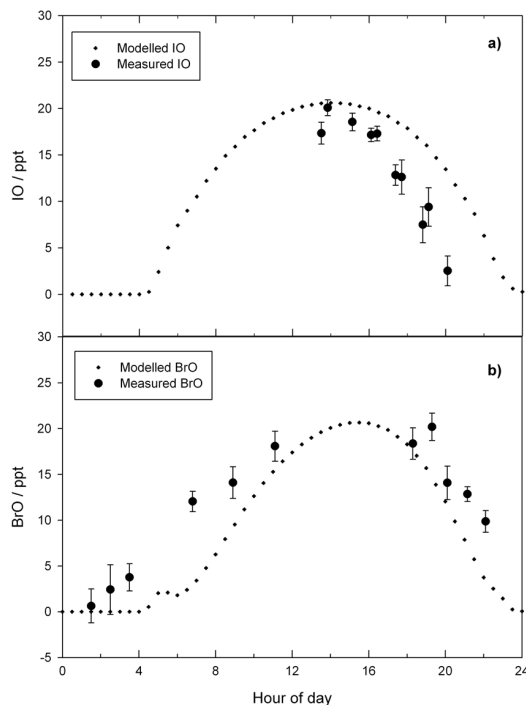

Fig. 5. Comparison of diurnal halogen oxides profiles at a height of 5 m measured by the DOAS instrument during the CHABLIS campaign and calculated using the revised model: **(a)** IO on 21 October 2004; **(b)** BrO on 20 October 2004.
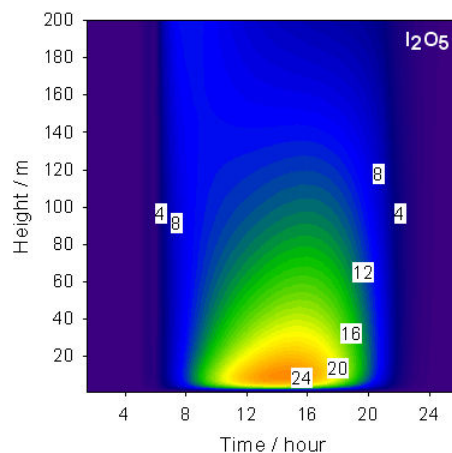

Fig. 6. Modelled diurnal I_2O_5 mixing ratio profile during the Antarctic springtime, using the revised model.

al., 2004; Saunders and Plane, 2006), there may be free energy barriers to the formation of small I_xO_y clusters which are not apparent at the relatively high concentrations of IO employed (compared with the atmosphere). The influence of humidity and other condensable vapours in the marine environment (e.g. H_2SO_4) also remains to be explored. Since there were no aerosol measurements during CHABLIS, we
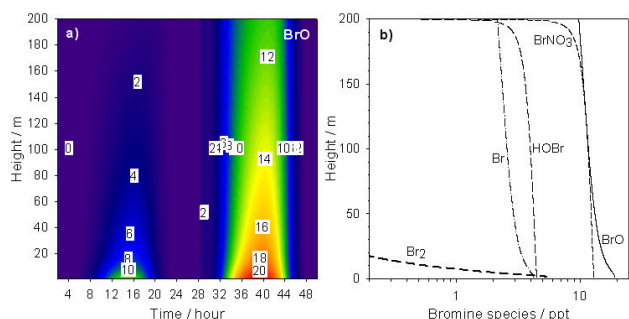
Fig. 7. (a) Two-day simulation of the boundary layer distribution of BrO during Antarctic springtime; **(b)** vertical profiles of the major gas-phase bromine species at noon on day 2. The mixing ratios at a height of 5 m agree well with the measurements made during the CHABLIS campaign using a DOAS with a beam ∼5 m above the snowpack (Saiz-Lopez, 2007a).

have not explicitly examined IOP production in this study, and IOP nucleation was not included in the model (i.e. I_2O_5 formation acts here as termination step for iodine chemistry in the standard model). It is worth noting that if polymerization is very rapid and without free energy barriers, then nucleation would compete with photolysis of I_xO_y, and an even larger iodine flux would be required to explain the IO observations.

IO was also observed at mixing ratios up to 6 ppt in air masses that had been over the continent for several days (Saiz-Lopez et al., 2007a). As mentioned earlier, this indicates an efficient iodine recycling mechanism capable of sustaining iodine radical chemistry over the snowpack. One possibility is the transport of sea-salt aerosol, and frost-flower fragments coated with sea-salt, from the ice front into the interior of the continent followed by deposition onto the snowpack; subsequent heterogeneous reactions would then recycle photolabile iodine to the gas phase, as we assume in THAMO. In fact, recent satellite measurements show that IO is widespread around coastal Antarctica, including areas over the snowpack (Saiz-Lopez et al., 2007b; Schönhardt et al., 2008). It is worth reiterating at this point that the sources of iodine are not well understood and hence in this study we have focused on finding the source strength of halogens needed, rather than on the nature of the source itself.

4.2 Bromine chemistry

Figure 7a shows a two-day model simulation of the BrO vertical profile in springtime. The initial Br_2 flux from the snowpack is set to be only 1×10^9 molecule $cm^{-2} s^{-1}$ (i.e. a factor of 5 smaller than the I atom flux (see above)), because of the effect of the bromine autocatalytic mechanism. It can be seen that on the second day of the simulation the BrO mixing ratios at the height of the DOAS measurements are similar to the observations, peaking at ∼20 ppt.

Figure 5b shows a comparison between the measured and modelled BrO at 5 m height. The observed diurnal asymmetry in the BrO is quite well reproduced by the model. During this season it is predicted that BrO will be better mixed within the boundary layer than IO (cf. Figs. 3 and 4). Figure 7b shows the noon vertical profiles of gas-phase bromine species during spring. Note that significant concentrations of inorganic bromine species reach the top of the BL, suggesting that BL ventilation under convective conditions may provide a source of inorganic bromine to the free troposphere. The predicted BrO column abundance for a 200 m BL height is 1×10^{13} molecule cm^{-2}, while satellite observations have reported averaged tropospheric vertical columns of 4×10^{13} molecule cm^{-2} in the austral spring over coastal Antarctica (Hollwedel et al., 2004). The difference could arise from the presence of a free tropospheric component in the satellite column measurement (Salawitch, 2006).

For the summertime case, a modelled BrO peak mixing ratio of 6 ppt at 4–5 m, in accord with the DOAS measurements, requires a Br_2 flux of 2×10^8 molecule $cm^{-2} s^{-1}$. For both summer and spring model runs the predicted concentrations essentially track the solar irradiance profile and therefore peak at local noon when photodissociation of photolabile bromine (e.g. Br_2, BrCl) is most efficient. In summer the BrO mixing ratio for SZA>90° does not decrease to zero since there is enough solar radiation reaching the surface during twilight for halogen activation to occur.

If heterogeneous reprocessing of bromine on sea-salt aerosol is switched off in the model, only a small fraction (∼10%) of BrO at the surface will be transported by convection to the top of the BL, producing a pronounced vertical gradient. In contrast, including heterogeneous processing of bromine yields a vertical distribution of BrO that is better mixed through the BL, in good accord with observations in the Arctic which have shown elevated levels of BrO at heights tens of meters above the snow surface (e.g. Tuckermann et al., 1997; Martinez et al., 1999; Hönninger et al., 2004a). This shows that aerosols have a significant effect on the vertical distribution of inorganic bromine, although the actual efficiency of the halogen aerosol processing will depend on the vertical profile of the aerosol size distribution and chemical composition (in particular, the degree of halide ion depletion and the pH of the aerosol). A final point is that although the model with heterogeneous processing predicts better vertical mixing for BrO, there is still a gradient in BrO measurements where the BrO mixing ratio at the top of the boundary layer is ∼50% lower than at the surface. This is in accord with observations of a negative vertical gradient in BrO reported by Avallone et al. (2003), where measurements of BrO in the Arctic were made using an in situ instrument near the surface (0.25–1 m) and a DOAS instrument higher up (20–200 m).

4.3 Impact of bromine and iodine chemistry on ozone

For a case where the noon peak of BrO is 10 ppt, a simple photochemical box model shows the diurnally-averaged O_3 loss rate is 0.14 ppb h^{-1} arising from bromine chemistry alone (the averaged background O_3 level during spring was $\sim$20 ppb). An O_3 depletion rate of 0.25 ppb h^{-1} is calculated for a noon peak of IO=10 ppt due to iodine chemistry only. When the halogens couple through the cross reaction

$$BrO + IO \rightarrow OIO + Br (R1a)$$

$$\rightarrow I + Br + O_2 \quad (R1b)$$
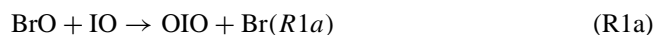
the total O_3 loss rate is 0.55 ppb h^{-1}, more than the sum of each component in isolation (Saiz-Lopez et al., 2007a). Thus, the O_3 depletion rate is almost four times as fast as that predicted from bromine chemistry alone, demonstrating the central role that iodine plays in O_3 depletion during Antarctic polar sunrise.

Figure 8a illustrates a THAMO run during springtime, for the case of a strong temperature inversion and stably buoyant BL, with no O_3 entrainment from the free troposphere. It can be seen that after 36 hours the computed O_3 levels in the BL drop to below the instrumental detection limit ($\sim$1 ppb) due to the combined impact of iodine and bromine chemistry. This is similar to the complete removal of O_3, which has been reported in the Arctic when a strong temperature inversion and high levels of BrO occur (e.g. Barrie et al., 1988; McConnell et al., 1992; Hönninger and Platt, 2002).

However, during the CHABLIS campaign it was observed that elevated levels of IO and BrO occurred without complete removal of O_3. We now use the THAMO model to examine whether the occurrence of high halogen oxide concentrations for a prolonged period of time without complete O_3 destruction can be explained by entrainment of O_3-rich air from aloft. Figure 8b shows the calculated O_3 profile with a downward flux from the free troposphere of O_3 of 3×10^{11} molecule cm^{-2} s^{-1}, and a convective BL. The predicted O_3 levels after 36 h have now only decreased by 20%, consistent with the observations (although after 48 hours the O_3 levels have decreased by $\sim$50%, so that significant O_3 does eventually occur). O_3 is well-mixed throughout the BL, without a pronounced vertical gradient, as observed by Arctic and Antarctic ozonesonde observations during ODEs (e.g. Wessel et al., 1998; Tarasick and Bottenheim, 2002).

Note that the model does not include a parameterization of BL ventilation. Hence, the halogen flux used in the model can be considered as a *lower limit* under convective boundary layer conditions. In addition to the difficulty of describing turbulent transport into the free troposphere, knowledge of halogen concentrations (and speciation) in the lower free troposphere is needed to properly quantify exchange with the BL, and the distribution of bromine and iodine in the free troposphere still remains an open question. Therefore, for a scenario with a prescribed halogen flux constant during each
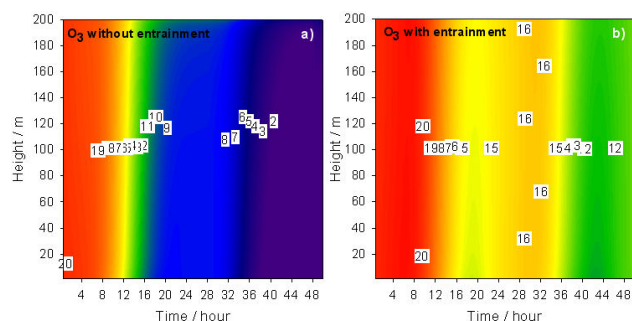

Fig. 8. Diurnal variation of the boundary layer O_3 profile in the presence of springtime BrO and IO levels for two scenarios: **(a)** no entrainment of O_3 and **(b)** entrainment of O_3 from the free troposphere.

sunlit period the model does not reach steady state, in part because BL ventilation is not included. However, an approach to steady-state conditions in the same air mass over several days is unlikely to occur in coastal Antarctica. A final point to consider here is an alternative explanation for the absence of complete O_3 destruction is the presence of high halogen concentrations. This is that air masses were being sampled where IO and BrO had been released so recently that significant O_3 depletion had not yet occurred. However, while this might explain the observations of O_3 and halogen oxides in air from the coastal sector, simultaneously high O_3 and halogen oxides were also seen in air masses that had been over the continent for several days (Saiz-Lopez et al., 2007a).

4.4 Impact of halogens on HO$_x$, NO$_x$ and the Hg lifetime

During January and February 2005 (austral summer), in situ measurements of OH and HO$_2$ were performed using the FAGE technique (Bloss et al., 2007). The measurements were made at the same height above the snowpack ($\sim$5 m) as the DOAS beam. Typical peak noon values of 4×10^{-2} ppt and 1.50 ppt were measured for OH and HO$_2$ respectively. IO and BrO react with HO$_2$ to form HOI and HOBr, whose subsequent photolysis produces OH, thus reducing the HO$_2$/OH ratio. In order to model the OH and HO$_2$ mixing ratios, we use the $J(O^1D)$ values measured during CHABLIS (typical noon photolysis frequency of 4×10^{-5} s^{-1}) and the measured mixing ratios of relevant species (see Sect. 2.2). Figure 9a and b show the effect of halogen chemistry on the vertical distributions of OH and HO$_2$, respectively, for runs with the standard model, the revised model, and no halogens. At the height of the measurements, the model runs without halogen chemistry over-predict HO$_2$ by $\sim$3 times the measured concentration, and underpredict OH by $\sim$40%. Thus, the modeled HO$_x$ (HO$_2$/OH) ratio is 115, compared with the measured ratio of 37. When halogen chemistry is included (i.e. typical summer noon BrO and IO mixing ratios of 5 ppt), the calculated OH and HO$_2$ levels and diurnal profile are in very
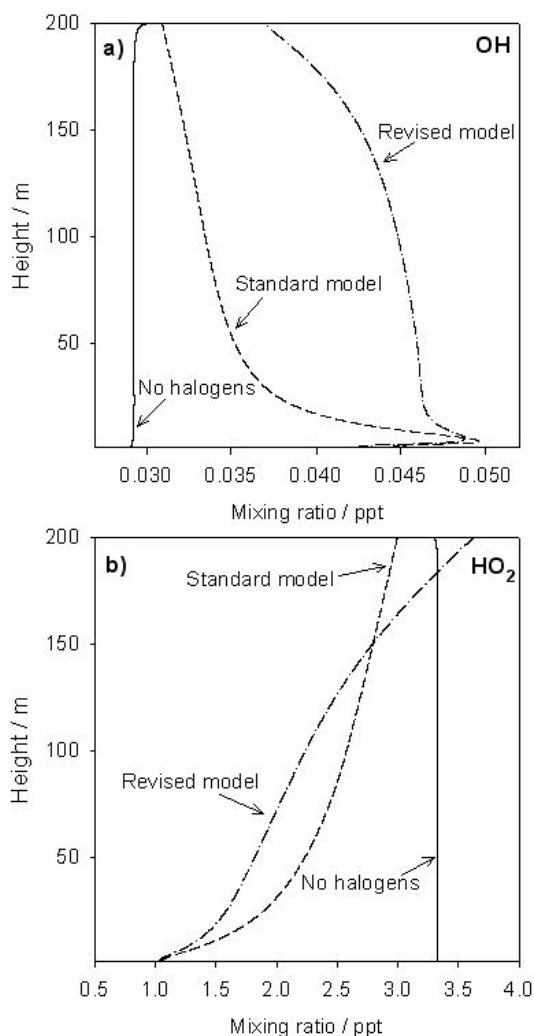
Fig. 9. Vertical profiles of **(a)** modelled OH and **(b)** modelled HO$_2$ for three scenarios: without halogen chemistry, with halogens (standard model), and including photolysis of I$_x$O$_y$ species (revised model).

good agreement with the observations: the modeled ratio is now 33. Figure 9 also shows that above about 10 m height there is a significant difference in the modeled OH and HO$_2$ profiles depending on whether I$_x$O$_y$ photochemistry is included.

NO and NO$_2$ were also measured during the Antarctic summer period with noon average mixing ratios of 14 ppt and 7.5 ppt, respectively, so that the NO$_x$ (NO$_2$/NO) ratio was 0.5. IO and BrO increase the NO$_2$/NO ratio by converting NO to NO$_2$. NO$_x$ is produced in the model by photochemistry of snowpack nitrate ions. The resulting summer and spring NO$_x$ fluxes from the snowpack were set to 2×10^8 and 1.2×10^7 molecule cm^{-2} s^{-1}, respectively, which were measured during CHABLIS (Jones et al., 2007b). Ventilation of NO$_x$ to the free troposphere, or entrainment from

the free troposphere into the BL, were not included. The model was constrained with summer J(NO$_2$) (typical noon maximum values of 0.015 s^{-1}) values measured with an actinic flux spectrometer during CHABLIS. Without halogens in the model, the NO$_x$ ratio at noon is only 0.3, whereas when halogens are included the ratio is 0.54.

Lastly, we use the measured XO concentrations and the XO:X ratio from THAMO to assess the impact of bromine and iodine chemistry on the lifetime of elemental mercury (Hg^0) over coastal Antarctica. To calculate the lifetime of Hg^0 against oxidation to Hg^{II}, we use the formalism given in Goodsite et al. (2004):

$$\tau = \frac{(k_{-2} + k_3[Br] + k_4[I])}{k_2[Br](k_3[Br] + k_4[I])} \quad (5)$$

where, at a pressure of 1 bar in air,

$$k(\text{Hg} + \text{Br} \rightarrow \text{HgBr}, \ 180-400 \text{ K}) =$$
$$1.1 \times 10^{-12}(T/298 \text{ K})^{-2.37} \text{ cm}^3 \text{ molecule}^{-1} \text{ s}^{-1} \quad (\text{R2})$$

$$k(\text{HgBr} \rightarrow \text{Hg} + \text{Br}, \ 180-400 \text{ K}) =$$
$$1.2 \times 10^{10} \exp(-8360/T) \text{ s}^{-1} \quad (\text{R-2})$$

$$k(\text{HgBr} + \text{Br} \rightarrow \text{HgBr}_2, \ 180-400 \text{ K}) =$$
$$1.4 \times 10^{-10} + 2.6 \times 10^{-13}.T - 8.6 \times 10^{-16}.T^2 \quad (\text{R3})$$

$$k(\text{HgBr} + \text{I} \rightarrow \text{HgBrI}, \ 180-400 \text{ K}) =$$
$$1.2 \times 10^{-10} + 4.2 \times 10^{-13}.T - 1.0 \times 10^{-15}.T^2 \quad (\text{R4})$$

During springtime, the model shows that the diurnally-averaged mixing ratio of BrO of ~8 ppt measured by DOAS would have coexisted in steady state with a Br mixing ratio of ~0.7 ppt for a springtime diurnally-averaged O$_3$ mixing ratio of 12 ppb. The computed lifetime of Hg^0, against oxidation by bromine chemistry alone (Reactions 2–3) is then about ~13 h at an average temperature of 260 K. The average IO measured by DOAS during springtime (~8 ppt) would have coexisted with a calculated I mixing ratio of ~5 ppt . The smaller IO/I ratio, compared to that of BrO/Br, arises from the self-reaction of IO to form OIO+I and I$_2$O$_2$ (Sander et al., 2006), and from the thermal decomposition of I$_2$O$_2$ to OIO+I and IO+IO. Including the role of atomic I through Reaction (R4) leads to a 40% reduction of the Hg lifetime. In addition, iodine chemistry decreases the calculated BrO/Br ratio from 11 to 5 via conversion of BrO back to Br through Reaction (R1).

The Hg^0 lifetime is predicted to be reduced to only 2 h under conditions of high XO mixing ratios (i.e. 20 ppt), as observed as Halley during springtime, when the Br and I mixing ratios would have been 4 ppt and 13 ppt, respectively. Note

that these calculations are made for high levels of halogens *without* severe O_3 depletion, as observed on occasions during CHABLIS (Saiz-Lopez et al., 2007a). If O_3 were completely removed, then the BrO/Br and IO/I ratios would decrease to 0.15 and 0.01, respectively, and the Hg^0 lifetime would be reduced to $\sim$10 min. Our measurements of BrO and IO therefore indicate that there should be sustained removal of Hg into the snowpack throughout the sunlit period in coastal Antarctica. Unfortunately, mercury measurements were not made during CHABLIS, but should certainly form a central component of any future campaigns in coastal Antarctica.

5 Summary and conclusions

The THAMO chemical transport model has been used to investigate the vertical gradients of halogens in the Antarctic coastal BL with a parameterization of the vertical transport under stable and convective BL conditions. The standard iodine chemistry model predicts a very steep gradient of iodine gas-phase species in the first 20 m of the BL. The result is that, although the predicted IO concentration at 5 m height is in good accord with the boundary layer DOAS observations during the CHABLIS campaign, the modelled column abundance is much less than the IO column abundance measured from ground-based and satellite-borne instruments. This indicates that IO is much better mixed in the BL than predicted by the standard model. We have therefore revised the standard model to including the photolysis of the higher iodine oxides I_2O_y, where y=2–5. These reactions recycle IO efficiently throughout the BL, producing much better agreement between the model and observations. The photochemistry of these species needs to be studied in the laboratory.

The revised THAMO model was then used to try and explain the surprising occurrence of close-to-average O_3 concentrations in the presence of high levels of IO and BrO. Within the constraints of a 1-D model, this can be achieved by replenishment of O_3 through entrainment from the free troposphere, to ensure that complete depletion of O_3 does not occur. The model then predicts a well-mixed vertical profile for O_3 within the BL, which is in agreement with ozonesonde observations. In some cases the simultaneous observation of high levels of halogen oxides and O_3 may also be explained by the very recent injection of the halogens into an air mass moving from the sea ice zone to Halley Bay.

The model is able to account for the measured perturbations in the HO_x and NO_x ratios by the observed concentrations of IO and BrO, and demonstrates that the presence of high atomic I concentrations leads to a significant enhancement in the oxidation rate of elemental Hg^0 by atomic Br.

Finally, the model requires very large fluxes of iodine precursors from the snowpack in order to account for the boundary layer observations of IO. This indicates an efficient recycling mechanism in the snowpack which is still to be understood.

References

Atkinson, R., Baulch, D. L., Cox, R. A., Crowley, J. N., Hampson, J., Hynes, R. G., Jenkin, M. E., Kerr, J. A., Rossi, M. J., and Troe, J.: Summary of evaluated kinetic and photochemical data for atmospheric chemistry, IUPAC, J. Phys. Chem. Ref. Data, 29, 167–266, 2000.

Avallone, L. M., Toohey, D. W., Fortin, T. J., McKinney, K. A., and Fuentes, J. D.: In situ measurements of bromine oxide at two high-latitude boundary layer sites: Implications of variability, J. Geophys. Res., 108, 4089, doi:10.1029/2002JD002843, 2003.

Barrie, L. A., Bottenheim, J. W., Schnell, R. C., Crutzen, P. J., and Rasmussen, R. A.: Ozone destruction and photochemical reactions at polar sunrise in the lower Arctic atmosphere, Nature, 334, 138–141, 1988.

Bloss, W. J., Lee, J. D., Johnson, G. P., Sommariva, R., Heard, D. E., Saiz-Lopez, A., McFiggans, G., Coe, H., Flynn, M., Williams, P., Rickard, A. R., and Fleming, Z. L.: Impact of halogen monoxide chemistry upon boundary layer OH and HO_2 concentrations at a coastal site, Geophys. Res. Lett., 32, L06814, doi:10.1029/2004GL022084, 2005.

Bloss, W. J., Lee, J. D., Heard, D. E., Salmon, R. A., Bauguitte, S. J.-B., Roscoe, H. K., and Jones, A. E.: Observations of OH and HO_2 radicals in coastal Antarctica, Atmos. Chem. Phys., 7, 4171–4185, 2007,
http://www.atmos-chem-phys.net/7/4171/2007/.

Bottenheim, J. W., Gallant, A. G., and Brice, K. A.: Measurements of NO_y Species and O_3 at 82° N Latitude, Geophys. Res. Lett., 13, 113–116, 1986.

Brooks, S. B., Saiz-Lopez, A., Skov, H., Lindberg, S. E., Plane, J. M. C., and Goodsite, M. E.: The mass balance of mercury in the springtime arctic environment, Geophys. Res. Lett., 33, L13812, doi:10.1029/2005GL025525, 2006.

Burkholder, J. B., Curtius, J., Ravishankara, A. R., and Lovejoy, E. R.: Laboratory studies of the homogeneous nucleation of iodine oxides, Atmos. Chem. Phys., 4, 19–34, 2004,
http://www.atmos-chem-phys.net/4/19/2004/.

Calvert, J. G. and Lindberg, S. E.: A modeling study on the mechanism of the halogen-ozone-mercury homogenous reactions in the troposphere during the polar spring, Atmos. Environ., 37, 4467–4481, 2003.

Calvert, J. G. and Lindberg, S. E.: Potential of iodine-containing compounds on the chemistry of the troposphere in the polar spring. I. Ozone depletion, Atmos. Environ., 38, 5087–5104, 2004a.

Calvert, J. G. and Lindberg, S. E.: Potential of iodine-containing compounds on the chemistry of the troposphere in the polar spring. II. Mercury depletion, Atmos. Environ., 38, 5105–5116, 2004b.

Courant, R., Friedrichs, K., and Lewy, H.: Über die partiellen Differenzengleichungen der mathematischen Physik, Mathematische Annalen, 100, 1, 32–74, 1928.

Davison, B., Hewitt, C. N., O'Dowd, C. D., Lowe, J. A., Smith, M. H., Schwikowski, M., Baltensperger, U., and Harrison, R. M.: Dimethyl sulphide, methane sulphonic acid and physicochemical aerosol properties in Atlantic air from the United Kingdom to Halley Bay, J. Geophys. Res., 101(D17), 22 855–22 868, 10.1029/96JD01166, 1996.

Evans, M. J., Jacob, D. J., Atlas, E., et al.: Coupled evolution of BrOx-ClOx-HOx-NOx chemistry during bromine-catalyzed ozone depletion events in the Arctic boundary layer, J. Geophys. Res., 108, 8368, doi:10.1029/2002JD002732, 2003.

Fickert, S., Adams, J. W., and Crowley, J. N.: Activation of Br_2 and BrCl via uptake of HOBr onto aqueous salt solutions, J. Geophys. Res.-Atmos., 104, 23 719–23 727, 1999.

Frieß, U., Wagner, T., Pundt, I., Pfeilsticker, K., and Platt, U.: Spectroscopic measurements of tropospheric iodine oxide at Neumayer Station, Antarctica, Geophys. Res. Lett., 28, 1941–1944, 2001.

Frieß, U., Hollwedel, J., Konig-Langlo, G., Wagner, T., and Platt, U.: Dynamics and chemistry of tropospheric bromine explosion events in the Antarctic coastal region, J. Geophys. Res., 109, D06305, doi:10.1029/2003JD004133, 2004.

Fuchs, N. A.: The mechanics of aerosols, Pergamon Press, New York, 1964.

Gomez Martin, J. C., Spietz, P., and Burrows, J. P.: Spectroscopic studies of the I_2/O_3 photochemistry – Part 1: Determination of the absolute absorption cross sections of iodine oxides of atmospheric relevance, J. Photochem. Photobio. A., 176, 15–38, 2005.

Gomez Martin, J. C., Spietz, P., and Burrows, J. P.: Kinetic and mechanistic studies of the I_2/O_3 photochemistry, J. Phys. Chem. A, 111, 306–320, 2007.

Goodsite, M. E., Plane, J. M. C., and Skov, H.: A theoretical study of the oxidation of Hg^0 to $HgBr_2$ in the troposphere, Environ. Sci. Technol., 38, 1772–1776, 2004.

Hoffmann, T., O'Dowd, C. D., and Seinfeld, J. H.: Iodine oxide homogeneous nucleation: An explanation for coastal new particle production, Geophys. Res. Lett., 28, 1949–1952, 2001.

Hollwedel, J., Wenig, M., Beirle, S., Kraus, S., Kuhl, S., Wilms-Grabe, W., Platt, U., and Wagner, T.: Year-to-year variations of spring time polar tropospheric BrO as seen by GOME, Adv. Space Res., 34, 804–808, 2004.

Hönninger, G., Leser, H., Sebastian, O., and Platt, U.: Ground-based measurements of halogen oxides at the Hudson Bay by active longpath DOAS and passive MAX-DOAS, Geophys. Res. Lett., 31(4), L04111, doi:10.1029/2003GL018982, 2004a.

Hönninger, G., von Friedeburg, C., and Platt, U.: Multi axis differential optical absorption spectroscopy (MAX-DOAS), Atmos. Chem. Phys., 4, 231–254, 2004b.

Hönninger, G. and Platt, U.: Observations of BrO and its vertical distribution during surface ozone depletion at Alert, Atmos. Environ., 36, 2481–2489, 2002.

Jimenez, J. L., Bahreini, R., Cocker, D. R., Zhuang, H., Varutbangkul, V., Flagan, R. C., Seinfeld, J. H., O'Dowd, C. D., and Hoffmann, T.: New particle formation from photooxidation of diiodomethane (CH_2I_2), J. Geophys. Res., 108, 4318, doi:4310.1029/2002JD002452, 2003.

Jones, A. E., Anderson, P. S., Wolff, E. W., Turner, J., Rankin,

A. M., and Colwell, S. R.: A role for newly forming sea ice in springtime polar tropospheric ozone loss?: Observational evidence from Halley Station, Antarctica, J. Geophys. Res., 111, D08306, doi:10.1029/2005JD006566, 2006.

Jones, A. E., Wolf, E. W., Salmon, R. A., et al.: Chemistry of the Antarctic boundary and the interference with Snow: an overview of the CHABLIS campaign, Atmos. Chem. Phys. Discuss., accepted, 2007a.

Jones, A. E., Wolff, E. W., Ames, D., Bauguitte, S. J.-B., Clemitshaw, K. C., Fleming, Z., Mills, G. P., Saiz-Lopez, A., Salmon, R. A., Sturges, W. T. and Worton, D. R.: The multi-seasonal NO_y budget in coastal Antarctica and its link with surface snow and ice core nitrate: results from the CHABLIS campaign, Atmos. Chem. Phys. Discuss., 7, 4127–4163, 2007b.

Joseph, D. M., Ashworth, S. H., and Plane, J. M. C.: On the photochemistry of $IONO_2$: absorption cross section (240–370 nm) and photolysis product yields at 248 nm, Phys. Chem. Chem. Phys., 5599–5607, doi:10.1039/b709465e, 2007.

Kaleschke, L., Richter, A., Burrows, J., Afe, O., Heygster, G., Notholt, J., Rankin, A. M., Roscoe, H. K., Hollwedel, J., Wagner, T., and Jacobi, H.-W.: Frost flowers on sea ice as a source of sea-salt and their influence on tropospheric halogen chemistry, Geophys. Res. Lett., 31, L16114, doi:10.1029/2004GL020655, 2004.

King, J. C. and Anderson, P. S.: Heat and water-vapor fluxes and scalar roughness lengths over and Antarctic ice shelf, Bound.-Lay. Meteorol., 69, 101–121, 1994.

Kreher, K., Johnston, P. V., Wood, S. W., Nardi, B., and Platt, U.: Ground-based measurements of tropospheric and stratospheric BrO at Arrival Heights, Antarctica, Geophys. Res. Lett., 24, 3021–3024, 1997.

Lehrer, E., Hönninger, G., and Platt, U.: A one dimensional model study of the mechanism of halogen liberation and vertical transport in the polar troposphere, Atmos. Chem. Phys., 4, 2427–2440, 2004,
http://www.atmos-chem-phys.net/4/2427/2004/.

Martinez, M., Arnold, T., and Perner, D.: The role of bromine and chlorine chemistry for Arctic ozone depletion events in Ny-Ålesund and comparison with model calculations, Ann. Geophys., 17, 941–956, 1999,
http://www.ann-geophys.net/17/941/1999/.

McConnell, J. C., Henderson, G. S., Barrie, L., Bottenheim, J. W., Niki, H., Langford, C. H., and Templeton, E. M. J.: Photochemical bromine production implicated in Arctic boundary-layer ozone depletion, Nature, 355, 150–152, 1992.

McFiggans, G., Plane, J. M. C., Allan, B. J., Carpenter, L. J., Coe, H., and O'Dowd, C.: A modeling study of iodine chemistry in the marine boundary layer, J. Geophys. Res., 105, 14 371–14 385, 2000.

McFiggans, G., Coe, H., Burgess, R., Allan, J., Cubison, M., Alfarra, M. R., Saunders, R., Saiz-Lopez, A., Plane, J. M. C., Wevill, D. J., Carpenter, L. J., Rickard, A. R., and Monks, P. S.: Direct evidence for coastal iodine particles from Laminaria macroalgae – linkage to emissions of molecular iodine, Atmos. Chem. Phys., 4, 701–713, 2004,
http://www.atmos-chem-phys.net/4/701/2004/.

Michalowski, B. A., Francisco, J. S., Li, S. M., Barrie, L. A., Bottenheim, J. W., and Shepson, P. B.: A computer model study of multiphase chemistry in the Arctic boundary layer during polar

sunrise, J. Geophys. Res., 105, 15 131–15 145, 2000.

Molina, M. J. and Rowland, F. S.: Stratospheric Sink for Chlorofluoromethanes – Chlorine Atomic-Catalysed Destruction of Ozone, Nature, 249, 810–812, 1974.

Murayama, S., Nakazawa, T., Tanaka, M., Aoki, S., and Kawaguchi, S.: Variations of tropospheric ozone concentration over Syowa Station, Antarctica, Tellus, 44B, 262–272, 1992.

O'Dowd, C. D., Geever, M., and Hill, M. K.: New particle formation: Nucleation rates and spatial scales in the clean marine coastal environment, Geophys. Res. Lett., 25, 1661–1664, 1998.

O'Dowd, C. D., Jimenez, J. L., Bahreini, R., Flagan, R. C., Seinfeld, J. H., Hameri, K., Pirjola, L., Kulmala, M., Jennings, S. G., and Hoffmann, T.: Marine aerosol formation from biogenic iodine emissions, Nature, 417, 632–636, 2002.

O' Driscoll, P., Lang, K., Minogue, N. and Sodeau, J.: Freezing halide ion solutions and the release of interhalogens to the atmosphere, J. Phys. Chem. A, 110(14), 4615–4618, 2006.

Oltmans, S. J. and Komhyr, W. D.: Surface Ozone Distributions and Variations from 1973-1984: Measurements at the NOAA Geophysical Monitoring for Climatic-Change Base-Line Observatories, J. Geophys. Res., 91, 5229–5236, 1986.

Plane, J. M. C. and Saiz-Lopez, A.: UV-Visible differential optical absorption spectroscopy (DOAS), in: Analytical techniques for atmospheric measurement, edited by: Heard, D. E., Blackwell Publishing, Oxford, 147–188, 2006.

Platt, U.: Differential optical absorption spectroscopy (DOAS), in: Air monitoring by spectroscopy techniques, edited by: Sigrist, M. W., John Wiley, London, 27–83, 1994.

Ramacher, B., Rudolph, J., and Koppmann, R.: Hydrocarbon measurements during tropospheric ozone depletion events: Evidence for halogen atom chemistry, J. Geophys. Res., 104, 3633–3653, 1999.

Read, K. A., Lewis, A. C., Salmon, R. A., Jones, A. E., and Bauguitte, S.: OH and halogen atom influence on the variability of nonmethane hydrocarbons in the Antarctic Boundary Layer, Tellus B, 59, 22–38, 2007.

Richter, A., Wittrock, F., Eisinger, M., and Burrows, J. P.: GOME observations of tropospheric BrO in Northern Hemispheric spring and summer 1997, Geophys. Res. Lett., 25, 2683–2686, 1998.

Richter, A., Wittrock, F., Ladstätter-Weißenmayer, A., and Burrows, J. P.: GOME measurements of stratospheric and tropospheric BrO, Adv. Space Res., 29, 1667–1672, 2002.

Saiz-Lopez, A. and Plane, J. M. C.: Recent applications of differential optical absorption spectroscopy: Halogen chemistry in the lower troposphere, J. de Physique IV, 121, 223–238, 2004a.

Saiz-Lopez, A. and Plane, J. M. C.: Novel iodine chemistry in the marine boundary layer, Geophys. Res. Lett., 31, L04112, doi:04110.01029/02003GL019215, 2004b.

Saiz-Lopez, A., Plane, J. M. C., and Shillito, J. A.: Bromine oxide in the mid-latitude marine boundary layer, Geophys. Res. Lett., 31, L03111, doi:10.1029/2003GL018956, 2004.

Saiz-Lopez, A., Plane, J. M. C., McFiggans, G., Williams, P. I., Ball, S. M., Bitter, M., Jones, R. L., Hongwei, C., and Hoffmann, T.: Modelling molecular iodine emissions in a coastal marine environment: the link to new particle formation, Atmos. Chem. Phys., 6, 883–895, 2006, http://www.atmos-chem-phys.net/6/883/2006/.

Saiz-Lopez, A., Mahajan, A. S., Salmon, R. A., Bauguitte, S. J.-B.,

Jones, A. E., Roscoe, H. K., and Plane, J. M. C.: Boundary layer halogens in coastal Antarctica, Science, 317, 348–351, 2007a.

Saiz-Lopez, A., Chance, K., Liu, X., Kurosu, T. P., and Sander, S. P.: First observations of iodine oxide from space, Geophys. Res. Lett., 34, L12812, doi:10.1029/2007GL030111, 2007b.

Salawitch, R. J.: Atmospheric chemistry: Biogenic bromine, Nature, 439, 275–277, 2006.

Sander, R., Vogt, R., Harris, G. W., and Crutzen, P. J.: Modeling the chemistry ozone, halogen compounds, and hydrocarbons in the Arctic troposphere during spring, Tellus, 49, 522–532, 1997.

Sander, S. P., Friedl, R. R., Ravishankara, A. R., Golden, D. M., Kolb, C. E., Kurylo, M. J., Huie, R., E., Orkin, V. L., Molina, M. J., Moortgart, G. K., and Finlayson-Pitts, B. J.: Chemical kinetics and photochemical data for use in atmospheric studies, Evaluation number 14, Jet Propulsion Laboratory and National Aeronautics and Space Administration, 2006.

Saunders, R. W. and Plane, J. M. C.: Formation pathways and composition of iodine ultra-fine particles, Environ. Chem., 2, 299–303, 2005.

Saunders, R. W. and Plane, J. M. C.: Fractal growth modelling of I_2O_5 nanoparticles, J. Aerosol Sci., 37, 1737–1749, 2006.

Schönhardt, A., Richter, A., Wittrock, F., Kirk, H., Oetjen, H., Roscoe, H. K., and Burrows, J. P.: Observations of iodine monoxide (IO) columns from satellite, Atmos. Chem. Phys., 8, 637–653, 2008, http://www.atmos-chem-phys.net/8/637/2008/.

Schroeder, W. H., Anlauf, K. G., Barrie, L. A., Lu, J. Y., Steffen, A., Schneeberger, D. R., and Berg, T.: Arctic springtime depletion of mercury, Nature, 394, 331–332, 1998.

Scott, K. J.: Bioavailable mercury in Arctic snow determined by a light-emitting mer-lux bioreporter, Arctic, 54, 92–95, 2001.

Sellegri, K., Loon, Y. J., Jennings, S. G., O'Dowd, C. D., Pirjola, L., Cautenet, S., Chen, H. W., and Hoffmann, T.: Quantification of coastal new ultra-fine particles formation from in situ and chamber measurements during the BIOFLUX campaign, Environ. Chem., 2, 260–270, 2005.

Shimazaki, T.: Minor constituents in the middle atmosphere, D. Reidel Publishing Company, Dordrecht, 1985.

Solberg, S., Schmidbauer, N., Semb, A., Stordal, F. and Hov, O.: Boundary-layer ozone depletion as seen in the Norwegian Arctic in Spring, J. Phys. Chem., 23, 301–332, 1996.

Spicer, C. W., Plastridge, R. A., Foster, K. L., Finlayson-Pitts, B. J., Bottenheim, J. W., Grannas, A. M., and Shepson, P. B.: Molecular halogens before and during ozone depletion events in the Arctic at polar sunrise: concentrations and sources, Atmos. Environ., 36, 2721–2731, 2002.

Stolarsky, R. and Cicerone, R. J.: Stratospheric Chlorine – Possible Sink for Ozone, Can. J. Chem., 52, 1610–1615, 1974.

Stull, R. B.: An introduction to boundary layer meteorology, Kluwer Academic Publishers, London, 1988.

Tarasick, D. W. and Bottenheim, J. W.: Surface ozone depletion episodes in the Arctic and Antarctic from historical ozonesonde records, Atmos. Chem. Phys., 2, 197–205, 2002, http://www.atmos-chem-phys.net/2/197/2002/.

Thompson, A. M.: The effect of clouds on photolysis rates and ozone formation in the unpolluted troposphere, J. Geophys. Res., 89, 1341–1349, 1984.

Tuckermann, M., Ackermann, R., Gölz, C., Lorenzen-Schmidt, H., Senne, T., Stutz, J., Trost, B. W., and Platt, U.: DOAS obser-

vation of halogen radical-catalysed Arctic boundary ozone destruction during the ARCTOC-campaigns 1995 and 1996 in Ny-Ålesund, Spitsbergen, Tellus, 49B, 533–555, 1997.

von Glasow, R., Sander, R., Bott, A., and Crutzen, P. J.: Modelling halogen chemistry in the marine boundary layer 1. Cloud-free MBL, J. Geophys. Res., 107, 4341, doi:10.1029/2001JD000942, 2002.

von Glasow, R. and Crutzen, P. J.: Tropospheric halogen chemistry, in: The Atmosphere, edited by: Keeling, R. F., Vol. 4, Treatise on Geochemistry, edited by: Holland, H. D. and Turekian, K. K., Elsevier-Pergamon, Oxford, 21–64, 2003.

von Glasow, R., von Kuhlmann, R., Lawrence, M. G., Platt, U., and Crutzen, P. J.: Impact of reactive bromine chemistry in the troposphere, Atmos. Chem. Phys., 4, 2481–2497, 2004, http://www.atmos-chem-phys.net/4/2481/2004/.

Wagner, T. and Platt, U.: Satellite mapping of enhanced BrO concentrations in the troposphere, Nature, 395, 486–490, 1998.

Wagner, T., Leue, C., Wenig, M., Pfeilsticker, K., and Platt, U.: Spatial and temporal distribution of enhanced boundary layer BrO concentrations measured by the GOME instrument aboard ERS-2, J. Geophys. Res., 106, 24 225–24 235, 2001.

Wessel, S., Aoki, S., Winkler, P., Weller, R., Herber, A., Gernandt, H., and Schrems, O.: Tropospheric ozone depletion in polar regions: A comparison of observations in the Arctic and Antarctic, Tellus, 50B, 34–50, 1998.